34th Annual International Conference of the IEEE EMBS
San Diego, California USA, 28 August - 1 September, 2012

Affine Transformation Registers Small Scale Lung Deformation

Tatsuya J. Arai[1,2], Christopher T. Villongco[1], Michael T. Villongco[2],
Susan R. Hopkins[2,3], and Rebecca J. Theilmann[3]

Abstract— **To evaluate the nature of small scale lung deformation between multiple pulmonary magnetic resonance images, two different kinematic intensity based image registration techniques: affine and bicubic Hermite interpolation were tested. The affine method estimates uniformly distributed deformation metrics throughout the lung. The bicubic Hermite method allows the expression of heterogeneously distributed deformation metrics such as Lagrangian strain. A cardiac triggered inversion recovery technique was used to obtain 10 sequential images of pulmonary vessel structure in a sagittal plane in the right lung at FRC in 4 healthy subjects (Age: 28.5(6.2)). One image was used as the reference image, and the remaining images (target images) were warped onto the reference image using both image registration techniques. The normalized correlation between the reference and the transformed target images within the lung domain was used as a cost function for optimization, and the root mean square (RMS) of image intensity difference was used to evaluate the quality of the registration. Both image registration techniques significantly improved the RMS compared with non-registered target images ($p = 0.04$). The spatial mean (μ_E) and standard deviation (σ_E) of Lagrangian strain were computed based on the spatial distribution of lung deformation approximated by the bicubic Hermite method, and were measured on the order of 10^{-3} or less, which is virtually negligible. As a result, small scale lung deformation between FRC lung volumes is spatially uniform, and can be simply characterized by affine deformation even though the bicubic Hermite method is capable of expressing complicated spatial patterns of lung deformation.**

Keywords: magnetic resonance imaging, image registration, lung mechanics, kinematic coordinate transformation.

I. Introduction

One advantage of using Magnetic Resonance Imaging (MRI) to study lung physiology is its flexibility: functional MR imaging gives the ability to probe respiratory physiology *in vivo*, provides structural information, and can provide multiple measures over several minutes since MRI does not require the administration of contrast agents or expose the subject to ionizing radiation. Our current functional MRI applications have focused on examining the spatial distribution of specific ventilation [1] and the temporal and spatial variability of pulmonary blood flow using dynamic arterial spin labeling imaging techniques [2, 3]. Both applications require images to be acquired every 5 seconds over the course of 15-30 minutes. During image aquisition, subjects are instructed to voluntarily gate their respiration so that images are acquired during a short breath-hold at a specified lung volume, typically functional residual capacity (FRC) [4]. However, this breathing maneuver can be difficult for some subjects and results in images acquired at lung volumes differing slightly from FRC. These registration errors can lead to measurement error and lower the quality of acquired physiological data. These errors may be significantly reduced if the appropriate registration techniques are employed.

Because the dynamics of lung deformation in one breathing cycle is mechanically nonlinear (i.e. the stress, strain, and mechanical properties of lung tissue are heterogeneously distributed [5, 6]), spatially flexible image registration techniques such as finite element interpolation method are required. However, we hypothesized that the deformation between MR lung images obtained at two different breath-holds at FRC (small scale lung deformation) will be uniformly distributed. To test this hypothesis we compared two image registraton techniques: affine (uniformly distributed axial and shear stretch, rotation, and translation throughout the lung) and bicubic Hermite (heterogeneously distributed deformation) registraton. The quality of image registration was assesed by the root mean square (RMS) of image intensity difference between reference and target images [7]. The nonlinearity of lung deformation was evaluated by examining the spatial heterogeneity of Lagrangian strain which is based on the resultant displacement field computed from the bicubic Hermite method.

A. MRI study

Four healthy male subjects participated in this study (Age: 28.5(6.2)). Each subject lay supine in a whole-body MR scanner (1.5 T GE HDx EXCITE twinspeed scanner). A torso coil was placed anterior and posterior to the subject's chest to maximize the signal to noise ratio. Each subject self-gated their respiratory cycle as 10 MR lung images were acquired over 50 seconds at FRC. A cardiac triggered inversion recovery sequence was used to acquire images of pulmonary vessel structure in a 15 mm thick sagittal slice in the right lung. The field of view was 40 cm × 40 cm with a resolution matrix of 256 × 256. An inversion time (T_I = 250-450 ms) was chosen for each subject to enhance the contrast between the blood entering the pulmonary vessel structure and the surrounding lung tissue. A chest belt was used to monitor the respiratory cycle, allowing the time of image acquisition to be synchronized with the breathing cycle and to ensure MR lung images were obtained at FRC (Fig. 1).

B. Image Registration

For each subject, one of the 10 images was chosen as a reference image. The deformation between the reference

Pulmonary Imaging Laboratory, Department of [1]Bioengineering, [2]Medicine, and [3]Radiology, Univ. of California, San Diego, 9500 Gilman Dr., La Jolla, CA 92093-0623A (e-mail: tarai@ucsd.edu).

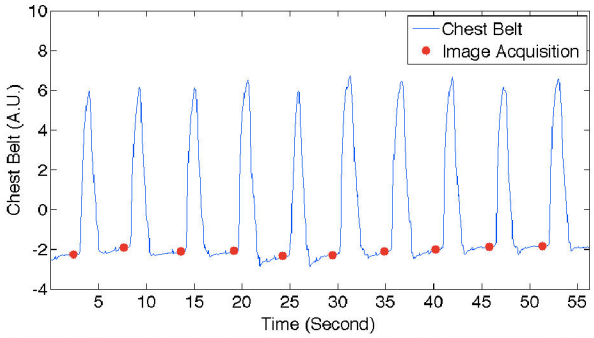

Figure 1. Chest belt signal and the timing of MR image acquisition (Subject 4). The blue solid line represents chest movement due to breathing as measured by an MR compatible belt wrapped around the subject's torso. The vertical axis shows an estimate of lung volume, and the bottom plateau represents the lung at FRC. MR image acquisition is denoted by a red dot.

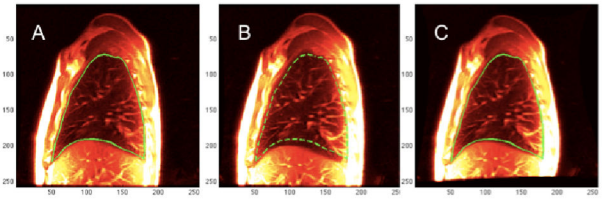

Figure 2. Image registration using bicubic Hermite transformation. A: Reference image acquired at FRC lung volume. The area encompassed by the green solid line is the manually drawn lung ROI. B: Representative target image acquired at a point in middle of a breathing cycle other than FRC (for demonstration). The green broken line represents the original lung ROI from the reference image, superimposed onto the target image. Misregistration between the reference image and the unregistered image within the green lines produced a poor normalized correlation of 0.772 (4). C: The coordinate transformation (bicubic Hermite interpolation) was applied to the target image in (B). For this example, the final registered image correlation was 0.972 (a 0.200 improvement). The root mean square (RMS) of signal intensity between reference and target images was originally 97.1, and improved to 73.6 with the image registration (5).

image and 9 remaining images (target/unregistered images) was computed by using two different kinematic coordinate transformation techniques: affine deformation (1) and bicubic Hermite interpolation (2,3)[8]. Affine deformation is manipulated by six different parameters for 2D coordinate transformation, whereas the bicubic Hermite method requires twenty-four parameters. Models with a large number of parameters can express the nonlinear spatial aspects of deformation. The bicubic Hermite interpolation method can compute the spatial variation of the deformation metrics (e.g. displacements, deformation gradients and strain fields), which are expected to be heterogeneously distributed throughout the lung. The advantage of this method is that it does not require assumptions about the spatial distribution of stress tensor and mechanical properties (Lamé constants) other than the implicit assumptions of continuum analysis.

Target images were warped onto the reference image by optimizing the corresponding parameters for each registration technique. A Nelder-Mead downhill simplex search method (implemented in MATLAB by the function fminsearch) was used for optimization to search for the best set of parameters. The normalized correlation (4)[9] between the reference images and the target image within a manually selected region of interest (ROI) was used as the cost function for the optimization (Fig.2. regions within green boundary). This process was repeated for each target image. Mathematical details for each registration technique are described in the appendix (sections A-C).

C. Data Analysis

The root mean square (RMS) within an ROI encompassing the entire lung (Fig. 2, regions within green boundary) between the reference image and the (un)registered images was used as a metric to evalute the quality of image registration (5). When two images are completely registered, RMS equals 0.0. The RMS was computed between the reference image and the following 3 groups: 1) 9 unregistered images, 2) 9 images registered with the affine deformation, and 3) 9 images registered with the bicubic Hermite interpolation. The results for each subject are presented in Table 1. ANOVA (Statview 5.0, SAS Institute, Cary, NC) for repeated measures was used to statistically evaluate differences between registration methods; The significance was accepted at a p-value < 0.05 (two-tailed).

The nonlinearity of lung deformation was further evaluated by examining the spatial distribution of Lagrangian strain (6), which was computed based on the transformation obtained using the bicubic Hermite method (Fig. 3). The mean Lagrangian strain (μ_E) over the lung ROI was used as an overall measure of lung deformation (i.e. the larger the absolute strain value, the larger the lung deformation, in which the positive sign represents inflation while the negative sign represents deflation). The standard deviation (σ_E) of Lagrangian strain was used as a metric of spatial heterogeneity of strain (larger σ_E, the more heterogeneous the spatial distribution of strain, whereas smaller σ_E indicates that the global lung deformation is homogeneous and can be characterized by affine lung deformation). Nine results of coordinate transformation (corresponding to 9 target images) were computed by bicubic Hermite method for each subject. Nine sets of Lagrangian strain maps (Fig.3 E_{11}, E_{12}, and E_{22}) were obtained for each subject. Then, 9 values of μ_E and 9 values of σ_E were computed from the three Lagrangian strain maps.

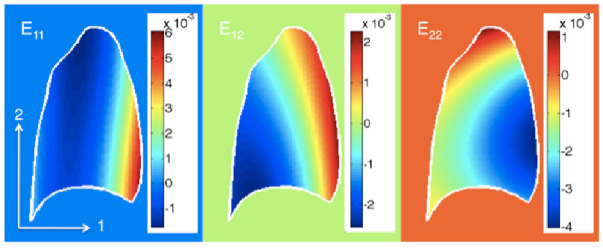

Figure 3. Representative maps of spatial distribution of Lagrangian strain (E_{11}, E_{12}, and E_{22}) between two FRC lung volumes (Subject 2). The white solid line represents the boundary of the lung ROI. Lagrangian strain was used as an index of nonlinear lung deformation and was computed from the coordinate transformation obtained from the bicubic Hermite finite element method (6). There are two perpendicular axes of deformation as represented by two arrows; 1: (Anterior – Posterior direction) and 2: (Superior – Inferior direction). The color bar represents the scale of the strain values and spatial variation of strain within the lung. The magnitude of strain values was on the order of 10^{-3}.

TABLE 1. Root mean square of intensity difference within the ROI

Subject	[1)]NonReg	Registration	
		[2)]Affine	[3)]Bicubic Hermite
#1	14.2(3.3)	11.8(1.5)	11.6(1.4)
#2	10.7(2.1)	9.8(1.8)	9.7(1.8)
#3	23.6(8.7)	17.1(3.6)	16.9(3.5)
#4	17.6(4.0)	15.8(3.1)	15.6(3.0)
Overall	16.5(5.5)*	13.6(3.4)	13.4(3.4)

Two different registration algorithms were compared; [1)] non registration, [2)] affine deformation and [3)] bicubic Hermite interpolation. The quality of registration are presented as mean(standard deviation) of 9 RMS values corresponding with 9 target images for each subject. The fifth row shows the overall effect, expressed as mean(standard deviation) across 4 subjects.
*Statistical significance in overall effect due to the registration, p= 0.04, ANOVA for repeated measures.

II. Results

A. Optimization of Image Registration

The values in the first column of Table 1 (RMS between the reference image and unregistered images) reflect the combined effects of the individual subject's ability to return FRC over time, the temporal and spatial noise within the MR image, and temporal fluctuations in pulmonary blood flow. As expected, the RMS between the reference image and the registered images was significantly improved for both methods when compared with non-registration ($p = 0.04$). Despite the fact that the bicubic Hermite method has larger degrees of freedom that allows for nonlinear deformation, this image registraton technique did not significantly outperform the affine registration method ($p = 0.86$).

B. Spatial Distribution of Lagrangian Strain

The results presented in Table 2 were expressed as mean(standard deviation) of spatial mean (μ_E) and mean(standard deviation) of spatial standard deviation (σ_E) of the Lagrangian strain over 9 coordinate transformation data for each subject. Since μ_E and σ_E are the order of 10^{-3} in both principal and shear directions, the effect of spatial heterogenity of lung deformation between two FRC lung volumes is mininal.

III. Discussion

The RMS results suggest that both affine and bicubic Hermite interpolation register images in similar way (the difference in RMS between affine and cubic Hermite was not statistically significant, p=0.86). The Lagrangian strain results suggest that the lung deformation between two different FRC lung volumes in separate breath-holds is small, and approximately homogeneous throughout the lung. Therefore, the nature of small scale lung deformation in separate breath-hold at FRC can be simply characterized by an affine deformation. Napadow et al. previously applied maps of the trace from grid tagging MRI during normal inspiration in healthy human subjects to quantify regional pulmonary strain tensor. Maximum and minimum trace values were reported to be 0.63 and -0.16, respectively, while maximum positive and negative shear strains were 0.42 and -0.20, respectively [5]. Compared to these values, the spatial mean (μ_E) and standard deviation (σ_E) of strains in our study are two orders of magnitudes smaller. This is an expected result for the healthy lung where the FRC volume is reproduceble in separate breath-holds, any small scale deformations between images are spatially homogeneous, and can be registered with an affine transformation.

However, in a diseased lung with an abnormal distribution of mechanical properties, e.g. chronic obstructive pulmonary disease, it is expected that the repeatability of obtaining the same FRC lung volume will be reduced. A more flexible image registration technique, e.g. bicubic Hermite method may need to be implemented to represent the deformation to minimize registration errors in the unhealthy lung.

The limitation of this work is the transformation is only applied in two-dimensions. However in a supine human, lung deformation occurs mainly in the superior – inferior (diaphragmatic motion) and the anterior – posterior directions (abdominal motion) while lateral expansion (rib cage motion) is negligible [10]. We believe our 2D implementation of image registration is sufficient to describe the small scale lung deformation as long as images are taken in sagittal plane.

Appendix

The initial coordinate system of the reference images is expressed as a_i. The target image coordinate system is expressed as x_i. Two different coordinate methods were compared: affine deformation (A) and bicubic Hermite finite element interpolation (B).

A. Affine Deformation

Affine deformation is defined by the following equation

$$x_i = F_{ij} a_j + b_i \tag{1}$$

F_{ij} is the deformation gradient matrix that defines axial and shear stretch, and rotation, while b_i is the translation vector. In a two-dimensional system, there are four elements in F_{ij}

TABLE 2. Spatial distribution of Lagrangian strain in lung: mean (μ_E) and standard deviation (σ_E) for each component of Lagrangian strain.

	E_{11} ($\times 10^{-3}$)		E_{22} ($\times 10^{-3}$)		E_{12} ($\times 10^{-3}$)	
	μ_E	σ_E	μ_E	σ_E	μ_E	σ_E
Subject 1	-1.96(2.02)	4.10(2.71)	1.81(4.74)	2.62(0.73)	1.17(2.22)	2.64(1.26)
Subject 2	0.73(0.96)	1.91(0.87)	0.57(1.93)	1.03(0.62)	-0.11(1.06)	1.37(0.59)
Subject 3	0.96(7.07)	3.35(2.09)	2.54(3.19)	2.86(1.70)	0.60(1.73)	3.61(2.39)
Subject 4	2.07(3.30)	6.00(3.01)	2.33(3.02)	2.71(1.68)	-0.70(1.18)	4.46(2.64)

One coordinate transformation results in one spatial mean (μ_E) and one spatial standard deviation (σ_E) of Lagrangian strain for each of three components. The data were expressed as mean(standard deviation) over nine coordinate transformation data for each subject from subject 1 to subject 4.

and two in b_i. A total of six parameters are required. The coordinate transformation computed by this method is spatially uniform.

B. Two Dimensional Finite Element Interpolation

The two dimensional finite element method of coordinate transformation is expressed by the following equation:

$$x_i = \sum n_{ik} \cdot \psi_{k1}\left(\xi_1(a_1)\right) \cdot \psi_{k2}\left(\xi_2(a_2)\right) \tag{2}$$

n_{ik} is the nodal parameter, ξ_j is the finite element coordinate system, and ψ_{kj} is the basis function. A single rectangular element is placed on the initial coordinate system, a_i, to encompass the lung region of interest in the reference image. The finite element coordinate system, ξ_j, ranges from 0 to 1 and is set within the element. ξ_j has a linear relationship with the initial coordinate system, a_j. The four corners of the element, i.e. ξ_j = [0, 0], [0, 1], [1,0], and [1,1], are assigned as nodes and each node has its own nodal parameters n_{ik}. The basis function ψ_{kj} is coupled with a corresponding node and its nodal parameter. The target image coordinate system x_i is thus expressed as the summation of the products of nodal parameters n_{ik} and basis functions ψ_{kj}. The transformation is only valid within the element.

For the bicubic Hermite interpolation, there are four basis functions.

$$\psi_0^0 = 2\xi^3 - 3\xi^2 + 1,\ \psi_1^0 = \xi^2(3 - 2\xi)$$
$$\psi_0^1 = \xi(\xi - 1)^2,\ \psi_1^1 = \xi^2(\xi - 1) \tag{3}$$

The subscript specifies the nodal location in the finite element coordinate. The superscript indicates the derivative of the nodal parameter n_{ik}; the basis function with the superscript 0 is coupled with the nodal parameter n_{ik}, whereas that with 1 is coupled with the partial derivative of the nodal parameter with respect to the finite element coordinate, $\partial n_{ik}/\partial\xi_1$ and $\partial n_{ik}/\partial\xi_2$. Therefore, each node has six nodal parameters for a total of 24 parameters to control this transformation. (Due to the minor impact on the calculation, eight terms with cross derivative, $\partial^2 n_{ik}/\partial\xi_1\partial\xi_2$, are ignored.) Since more numbers of nodal parameters enable larger degrees of freedom, this transformation method is able to approximate the more complex spatial aspects of lung deformation.

C. Image Registration

The normalized correlation between the reference and transformed target images within the lung region of interest was used as the cost function. A correlation coefficient close to 1.0 represents completely optimized image registration.

$$R = \frac{\sum\left(I_{ref}(A_i) - \hat{I}_{ref}\right)\left(I_{tar}(x_j(A_i)) - \hat{I}_{tar}\right)}{\sqrt{\sum\left(I_{ref}(A_i) - \hat{I}_{ref}\right)^2 \sum\left(I_{tar}(x_j(A_i)) - \hat{I}_{tar}\right)^2}} \tag{4}$$

I_{ref} is the reference image in which the signal intensity is corrected by the determinant of deformation gradient matrix, F_{ij} i.e. the determinant of Jacobian matrix. Since MR signal intensity is proportional to the proton density, the voxel size change due to the deformation must be considered. I_{tar} is the target image. A_i is the pixel coordinate within the lung ROI expressed along the initial coordinate system a_i. $I_{ref}(A_i)$ and I_{target} $(x_j(A_i))$ are therefore the spatially coupled signal intensity map of the reference image and transformed target image within the lung. $\hat{I}_{ref}$ and $\hat{I}_{tar}$ are mean signal intensity along the lung domain within I_{ref} and I_{tar}, respectively.

D. Root Mean Square (RMS) of Signal Intensity Difference

The root mean square of signal intensity difference is used as a metric to evaluate the quality of image registration.

$$RMS = \sqrt{\frac{\left(I_{ref}(A_i) - I_{tar}(x_j(A_i))\right)^2}{N}} \tag{5}$$

in which N is the number of voxels within the lung ROI.

E. Lagrangian Strain

The Lagrangian E_{KL} strain is expressed as,

$$E_{KL} = \frac{1}{2}\left(F_{iK}F_{iL} - I_{KL}\right) \tag{6}$$

in which F_{ij} is deformation gradient matrix and I_{kL} is the identity matrix. Four components of Lagrangian strain are defined in two-dimension, E_{11}, E_{22}, E_{12} and E_{21}. Because of symmetry, E_{12} and E_{21} are identical. E_{11} and E_{22} are indices of principal stretch along the principal axes, while E_{12} represents for shear.

ACKNOWLEDGMENT

The authors thank Dr. Mithun Diwakar and Dr. Rui Carlos Sá for the technical help as well as for discussions.

REFERENCES

[1] R.C. Sa, M.V. Cronin, A.C. Henderson, S. Holverda, R.J. Theilmann, T.J. Arai, D.J. Dubowitz, S.R. Hopkins, R.B. Buxton, and G.K. Prisk, "Vertical distribution of specific ventilation in normal supine humans measured by oxygen-enhanced proton MRI," *J Appl Physiol*, vol. 109, (no. 6), pp. 1950-9, Dec.

[2] D.S. Bolar, D.L. Levin, S.R. Hopkins, L.F. Frank, T.T. Liu, E.C. Wong, and R.B. Buxton, "Quantification of regional pulmonary blood flow using ASL-FAIRER," *Magn Reson Med*, vol. 55, (no. 6), pp. 1308-17, Jun 2006.

[3] A.C. Henderson, G.K. Prisk, D.L. Levin, S.R. Hopkins, and R.B. Buxton, "Characterizing pulmonary blood flow distribution measured using arterial spin labeling," *NMR Biomed*, vol. 22, (no. 10), pp. 1025-35, Dec 2009.

[4] T.J. Arai, G.K. Prisk, S. Holverda, R.C. Sa, R.J. Theilmann, A.C. Henderson, M.V. Cronin, R.B. Buxton, and S.R. Hopkins, "Magnetic resonance imaging quantification of pulmonary perfusion using calibrated arterial spin labeling," *J Vis Exp*, (no. 51).

[5] V.J. Napadow, V. Mai, A. Bankier, R.J. Gilbert, R. Edelman, and Q. Chen, "Determination of regional pulmonary parenchymal strain during normal respiration using spin inversion tagged magnetization MRI," *J Magn Reson Imaging*, vol. 13, (no. 3), pp. 467-74, Mar 2001.

[6] T.A. Sundaram and J.C. Gee, "Towards a model of lung biomechanics: pulmonary kinematics via registration of serial lung images," *Med Image Anal*, vol. 9, (no. 6), pp. 524-37, Dec 2005.

[7] L.C. Maas and P.F. Renshaw, "Post-registration spatial filtering to reduce noise in functional MRI data sets," *Magn Reson Imaging*, vol. 17, (no. 9), pp. 1371-82, Nov 1990.

[8] P.M. Nielsen, I.J. Le Grice, B.H. Smaill, and P.J. Hunter, "Mathematical model of geometry and fibrous structure of the heart," *Am J Physiol*, vol. 260, (no. 4 Pt 2), pp. H1365-78, Apr 1991.

[9] D.L. Hill, P.G. Batchelor, M. Holden, and D.J. Hawkes, "Medical image registration," *Phys Med Biol*, vol. 46, (no. 3), pp. R1-45, Mar 2001.

[10] S.J. Cala, J. Edyvean, and L.A. Engel, "Abdominal compliance, parasternal activation, and chest wall motion," *J Appl Physiol*, vol. 74, (no. 3), pp. 1398-405, Mar 1993.